

# Dynamical properties of the compounds $\text{CuGeO}_3$ and $\alpha'$ - $\text{NaV}_2\text{O}_5$ at temperatures $T \neq 0$ .

K. Fabricius

*Physics Department, University of Wuppertal, 42097 Wuppertal*

U. Löw

*Physikalisches Institut der Johann Wolfgang Goethe Universität, D-60054 Frankfurt am Main, Germany*

(October 25, 2018)

The dynamical structure factor of the frustrated spin 1/2 Heisenberg model for a series of frustration parameters at finite temperatures is presented. A sharp upper boundary of the spinon continuum is found. A simple method to extract the nearest neighbour coupling  $J$  from the spectral width is suggested. Signatures of frustration are discussed and a comparison with neutron inelastic scattering data is given.

PACS numbers: 75.10.Jm, 75.40.Gb, 75.40.Mg, 75.50.Ee

The recent widespread interest in low-dimensional quantum spin systems has been brought up and maintained by the discovery of new compounds with a variety of spin-spin couplings. Particular effort has been concentrated on the first two inorganic substances undergoing a Spin-Peierls transition:  $\text{CuGeO}_3$  and  $\alpha'$ - $\text{NaV}_2\text{O}_5$ .

There is extensive literature on the low temperature properties of  $\text{CuGeO}_3$  (see for example Ref. [1] and references therein), but there is still no agreement on the model describing the uniform phase ( $T > T_{SP}$ ) also. If the interchain interaction is negligible the most likely candidate is the isotropic frustrated spin 1/2 Heisenberg model [2,3] in one dimension

$$H = 2J \sum_{i=1}^N \left\{ \vec{S}_i \cdot \vec{S}_{i+1} + \alpha \vec{S}_i \cdot \vec{S}_{i+2} \right\}. \quad (1)$$

Alternatively Uhrig proposed a model including interchain interaction with a small value of inchain next to nearest neighbour coupling  $\alpha$  [4].

In a recent study [5] it has been demonstrated compellingly that in the framework of the first model (Eq. (1)) for the unique set of parameters  $J/k_B = 80K$  and  $\alpha = 0.35$  excellent agreement between experiment and theory is achieved for the magnetic susceptibility.

In the following we focus on the dynamical properties of both substances at temperatures  $k_B T \geq 0.6J$ . We compare our theoretical results with data obtained from neutron inelastic scattering (NIS) experiments [6] performed on  $\text{CuGeO}_3$ . There are still no corresponding results for  $\alpha'$ - $\text{NaV}_2\text{O}_5$ . If it is confirmed that  $\alpha'$ - $\text{NaV}_2\text{O}_5$  is well described by the pure isotropic Heisenberg model our results for  $\alpha = 0$  can be taken as a prediction for this compound.

We have determined the dynamic structure factor  $S(q, \omega)$  at finite  $T$  for the frustrated Heisenberg model

and the  $XXX$ -model for chains with  $N = 16, 18$  spins and periodic boundary conditions by the method of complete and exact diagonalization (CED) as described in detail in Ref. [7]. This was done for  $\alpha = 0.0, 0.06, 0.12, 0.18, 0.24, 0.35, 0.45, 0.5$ . The largest subspaces to be treated are of dimension 415 for  $N = 16$  and 1367 for  $N = 18$  (see also Ref. [8]). Our aim is to study the dependence of  $S(q, \omega)$  on the frustration parameter  $\alpha$  at  $T \neq 0$  and to highlight the unambiguous features distinguishing models with varying degree of frustration.

We study chains with maximal 18 spins. Lanczos studies of ground state properties of spin  $\frac{1}{2}$  systems routinely handle chains of 30 spins. So one could dismiss the present work as not worthwhile because it is expected to be too inaccurate. But thermodynamical observables can be determined by CED with high accuracy for temperatures  $k_B T \geq 0.6J$ . An extensive investigation of finite size errors of dynamical correlations convinced us that this method, if carefully applied, gives sufficiently accurate results with easily controllable errors, which are not obscured by more or less arbitrary approximations. The obvious reason is that the number of contributing matrix elements is for  $T > 0$  many orders of magnitude larger than for  $T = 0$ . We refer to Ref. [7] where a thorough finite size analysis is presented and to remarks in the course of this paper. With substantially more effort marginally longer chains could be studied exactly. But probably the additional accuracy would barely justify the effort. The real challenge is instead to extract as much reliable results as possible from the existing data.

For  $k_B T < 0.6J$  the method applied by us gives only poor results. We therefore restricted ourselves to temperatures  $k_B T \geq 0.6J$  and considered qualitative and global features respectively. For higher temperatures where our method is accurate the existing experimental results are of qualitative nature only and our data can serve in the

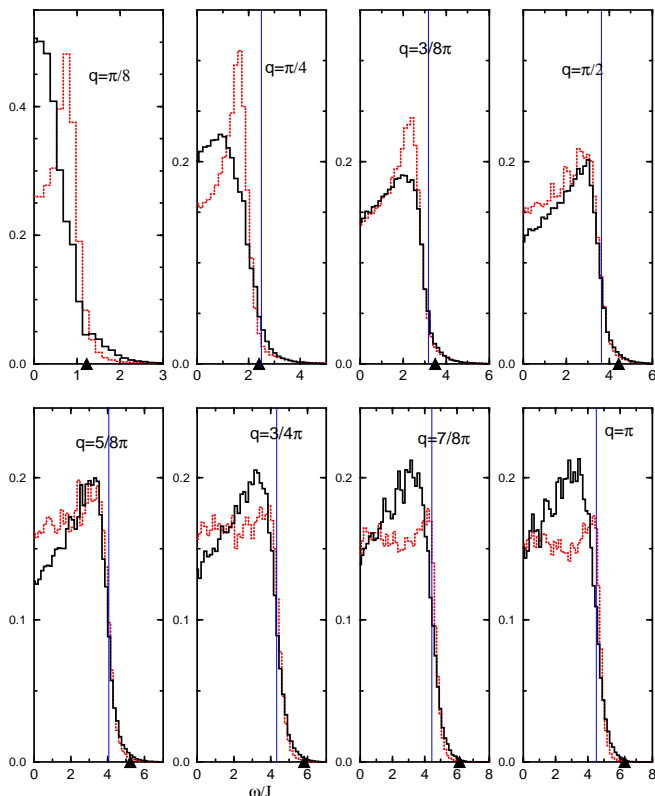


FIG. 1. Dynamical structure factor for  $\alpha = 0.0$  (black solid line) and  $\alpha = 0.35$  (red dashed line), as a function of  $\omega/J$  for  $k_B T = 3.8J$ . The triangles mark the upper boundary of the two-spinon continuum for the XXX-model. The blue vertical lines mark the experimental spectral boundaries read off from Fig.4 in Ref. [6].

future to disentangle magnetic and phononic contributions in the analysis of experimental data.

We find that the structure function has for all practical purposes (but not strictly) a bounded support in the  $q - \omega$  plane. The lower boundary - well known from spin dynamics at  $T = 0$  - disappears gradually for growing  $T$  (see Figs.1, 2), whereas the upper boundary is nearly unchanged up to infinite temperature. The structure function develops for increasing  $T$  a steep slope at its boundary. We emphasize that the boundary as well as the functional form of  $S(q, \omega)$  near the boundary determined by CED show very small finite size errors: While the precise positions of local peaks of  $S(q, \omega)$  for small and intermediate  $\omega$  are not perfectly  $N$ -independent for small  $T$ , the shape near the boundary and the location of the boundary are remarkably stable. In any case the spectral boundary is easily determined independently of the criteria applied. This is in sharp contrast to the situation at  $T = 0$  where the standard tool to study spin dynamics is the recursion method [9], which works well for low lying excitations but is much less accurate for higher ones.

It is a remarkable and unexpected result that for  $T > 0$  the spectral density is bounded by a curve similar (but

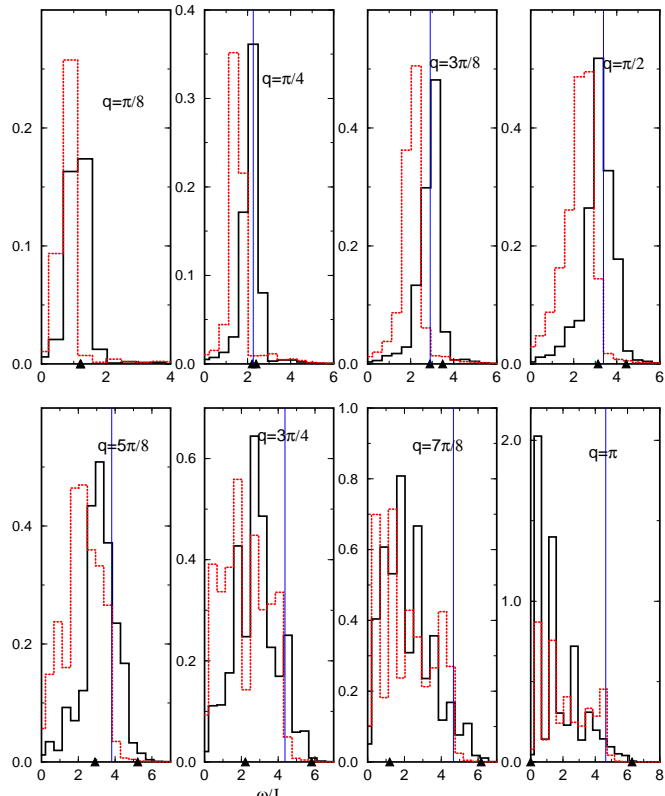


FIG. 2. As Fig.1 but for  $k_B T = 0.6J$ . The triangles mark the upper and lower boundaries of the two-spinon continuum for the XXX-model. The blue vertical lines mark the experimental spectral boundaries read off from Fig.1b in Ref. [6].

not equal) to the two spinon boundary of  $S(q, \omega)$  in the XXX-model detected by Müller et al. [10] at  $T = 0$ . For  $T \geq 0$  this was first observed in Ref. [7].

As for  $T = 0$  this results from a suppression of the matrix elements  $|\langle \nu | S_3(q) | \mu \rangle|$  for large energy transfer. The density of allowed pairs of excitations however is not responsible for the steep drop of  $S(q, \omega)$  near the boundary since it is still sizable for values of the energy transfer far beyond the boundary of the two-spinon continuum. This is shown in Fig. 3 for  $\alpha = 0.0, 0.35$ .

The spinon is a rigorously defined notion only in the context of exactly solvable models (ESM) where Bethe- Ansatz techniques work [11–17]. It is indispensable to understand the physics of spin dynamics at  $T = 0$  as first noted and discussed exhaustively in [13], see also [18,19]. As we have just demonstrated, certain aspects of spin dynamics at  $T = 0$  in ESM and  $T > 0$  ( up to infinite temperature ) even for not exactly solvable models are strikingly similar. This makes it evident that the spinon is a much broader concept than originally anticipated.

Our most conspicuous new result is shown in Figs. 1, 2,4: the spectral width is essentially independent of  $\alpha$  for  $q = \pi$ . This is of eminent importance for the analysis of experiments: it allows to determine the coupling  $J$  and its temperature dependence from neutron inelastic scattering without any further assumption on the model

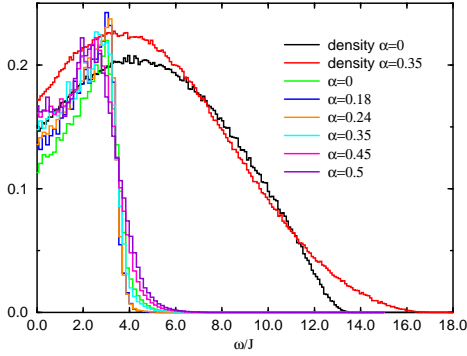


FIG. 3.  $S(q = \pi/2, \omega)$  for  $\alpha = 0.0, 0.18, 0.24, 0.35, 0.45, 0.5$  at  $k_B T = 3.2J$  and the density of contributing excitations for  $\alpha = 0$  and  $\alpha = 0.35$  (rescaled).

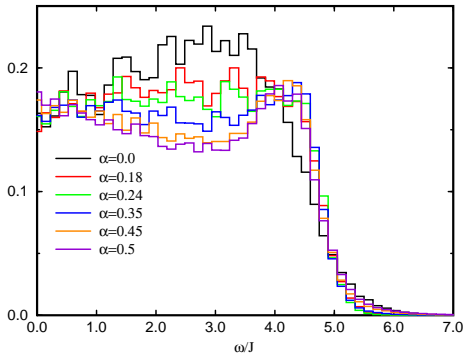


FIG. 4.  $S(q = \pi, \omega)$  for  $\alpha = 0.0, 0.18, 0.24, 0.35, 0.45, 0.50$  and  $k_B T = 3.2J$ .

parameters.

A similar statement can be made about the normalized integrated intensity

$$\Sigma(q, \omega) = \frac{1}{S_\infty(q)} \int_0^\omega S(q, \omega') d\omega' \quad (2)$$

with  $S_\infty(q) = \int_0^\infty S(q, \omega') d\omega'$ . For  $q = \pi$  there exists for each temperature an interval where these functions are narrowly coalescing for all  $\alpha$  values ( see e.g. Fig. 5).

Arai et al. [6] measured a spectral width of 32 meV at  $T = 50K$ . This gives  $J/k_B = 79K$  and is in perfect agreement with  $J/k_B = 80K$  determined from the observation that the magnetic susceptibility has its maximum at  $T = 56K$  [5]. So we observe that completely independent experiments performed in the same energy range give the same value for the coupling  $J$ . At  $T = 300K$  the measured width is 30 meV corresponding to  $J/k_B = 68K$ .

Having determined  $J$  by this very simple method, we

obtain the value of  $\alpha$  from finer details of  $S(q, \omega)$ . These are:

(i) The theoretical width of the spectral density for  $q \neq \pi$  shows for low temperatures a distinct  $\alpha$ -dependence. We extracted the boundary of the spectral density from the color contour maps of Ref. [6]. They are shown as vertical lines in Fig. 1 and 2. For  $T = 50K$  they coincide perfectly with the theoretical result valid for  $\alpha = 0.35$ .

(ii) The integrated intensity  $S_\infty(q)$  is shown in Fig.6 for  $T = 50K$  in conjunction with data from Arai et al. (see Fig. 2 of Ref. [6]). If the vertical scale of the experimental data is appropriately adjusted the agreement of experiment and theory is remarkable for  $\alpha \approx 0.35$ , whereas  $\alpha = 0$  is clearly ruled out. There is no question of finite-size errors, they are much smaller than the experimental errors as shown in the figure.

(iii) A further distinguishing qualitative feature is the trough-shaped structure detected experimentally which is fully developed at  $T = 300K$  (see Fig.4 of Ref. [6]). Fig. 4 shows that the same phenomenon is present for  $\alpha \geq 0.35$  whereas for  $\alpha = 0$  we find a hill-like structure.

Summarizing we have found an unexpected high degree of correspondence of experimental data and theoretical results. We state that the model parameters  $J$  and  $\alpha$  obtained from thermodynamical properties of  $\text{CuGeO}_3$  are also strongly favoured by NIS data.

We conclude this section by predicting some properties of the NIS cross-section of  $\alpha'$ - $\text{NaV}_2\text{O}_5$ . Assuming  $\alpha = 0$  we find :

1.) The spectral boundary  $\omega_B \pm \Delta\omega_{L,R}$  for  $k_B T = 1.2J$  and  $q = m\pi/8$  is given in the following table. Here  $\Delta\omega_R$  is much larger than  $\Delta\omega_L$ , because  $S(q, \omega)$  for  $\alpha = 0$  has a flat tail and becomes steeper for larger temperatures only.

m	$\omega_B/J$	$\Delta\omega_L/J$	$\Delta\omega_R/J$
1	2.04	0.16	0.60
2	2.78	0.14	1.37
3	3.84	0.43	1.33
4	4.76	0.46	1.20
5	5.22	0.48	0.77
6	5.51	0.58	0.60
7	5.95	0.44	0.32
8	5.65	0.43	0.76

2.) The integrated spectral density  $S_\infty(q)$  at  $k_B T = 0.6J$  is shown in Fig. 6 for  $\alpha = 0$ .

3.) In clear distinction to  $\text{CuGeO}_3$  the intensity is not suppressed but enhanced around  $\omega/J = 3$  and  $q = \pi$ .

For a discussion of the underlying physics we refer to Ref. [7]. We add the following supplement. As we consider here solely isotropic models the spin  $\vec{S}$  is conserved and we can study another classification of excitations contributing to  $S(q, \omega)$ . There are two classes of transitions behaving markedly different:

1.)  $\Delta S = 0$  transitions: They do not occur for  $T = 0$ . In Fig. 7 it is shown that they contribute mainly to the central bulk of  $S(q, \omega)$ .

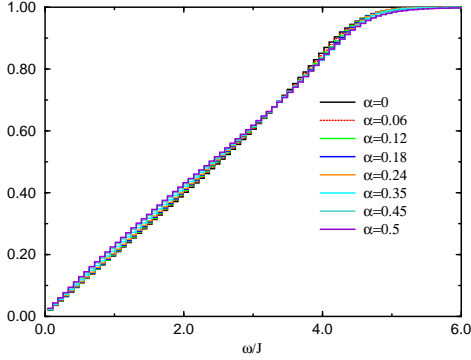


FIG. 5.  $\Sigma(q = \pi, \omega, T = \infty)$  for  $N = 16$  and  $\alpha=0.0, 0.06, 0.12, 0.18, 0.24, 0.35, 0.45, 0.5$ .

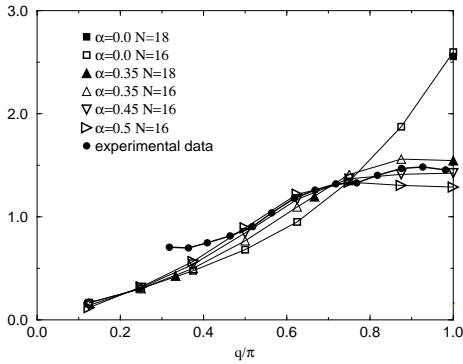


FIG. 6.  $S_\infty(q)$  at  $k_B T = 0.6J$  for  $\alpha = 0.0, 0.35, 0.45, 0.5$  for  $N = 16, 18$  and experimental data at  $T = 50K$  read off from Fig.2 in Ref. [6]. (The lower limit of integration for the theoretical curves is 3meV with  $J/k_B = 80K$  in accordance with Ref. [6].)

2.)  $\Delta S = 1$  transitions: Besides adding intensity to the central region they build up the steep slope near the spectral boundary.

This note is exclusively devoted to an attempt to explain NIS data of  $\text{CuGeO}_3$  in the framework of model Eq. (1). We postpone other topics like a theoretically oriented study of spin dynamics in frustrated models as well as the application to e.g. Raman scattering to future publications.

We are grateful to M.Arai and M.Fujita for comments on their NIS data. We thank A. Fledderjohann, M. Karbach and K.-H. Mütter for discussions on spin dynamics at low temperatures. U.L. gratefully thanks B. Lüthi for stimulating discussions and support and M. Braden for information on NIS.

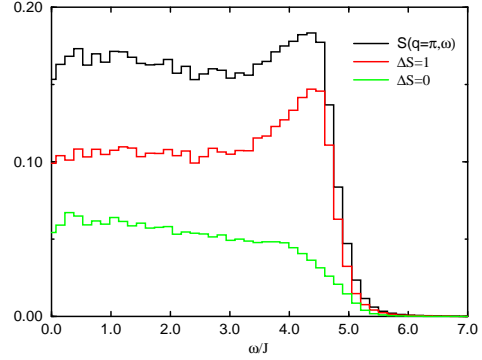


FIG. 7.  $S(q = \pi, \omega)$  at  $k_B T = 3.2J$  for  $N = 18$  and  $\alpha = 0.35$ . Contribution from transitions with  $\Delta S = 0$  and  $\Delta S = 1$

- 
- [1] D. Augier, D. Poilblanc, S. Haas, A. Delia and E. Dagotto, Phys. Rev. B **56**, R5732 (1997).
  - [2] G. Castilla, S. Chakravarty and V. J. Emery, Phys. Rev. Lett. **75**, 1823 (1995).
  - [3] J. Riera and A. Dobry, Phys. Rev. B **51**, 16098 (1995).
  - [4] G. Uhrig, Phys. Rev. Lett. **79**, 163 (1997).
  - [5] K. Fabricius, A. Klümper, U. Löw, B. Büchner, G. Dhalenne, T. Lorenz, A. Revcolevschi cond-mat 9705036.
  - [6] M. Arai, M. Fujita, M. Motokawa, J. Akimitsu, and S.M. Bennington, Phys. Rev. Lett. **77**, 3649 (1996).
  - [7] K. Fabricius, U. Löw, J. Stolze, Phys. Rev. B **55**, 5833 (1997).
  - [8] O.A. Starykh, A.W. Sandvik, R.R.P. Singh Phys. Rev. B. **55**, 14953 (1997).
  - [9] V.S.Viswanath, Gerhard Müller, The Recursion Method, Springer.
  - [10] G. Müller, H. Thomas, M. Puga, and H. Beck, J. Phys. C (Cond. Mat.) **14**, 3399 (1981).
  - [11] T. Yamada, Prog. Theor.Phys. **41**, 880 (1969).
  - [12] J. D. Johnson, S. Krinsky, B. McCoy Phys. Rev. A **8**, 2526 (1973).
  - [13] G. Müller, H. Thomas, H. Beck, and J.Bonner, Phys. Rev. B **24**, 1429 (1981).
  - [14] L.D. Faddeev and L.A. Takhtajan, Phys. Lett. **85A**, 375 (1981).
  - [15] F.D.M. Haldane, Phys. Rev. Lett. **60**, 635 (1988).
  - [16] B.S. Shastry, Phys. Rev. Lett **60**, 639 (1988).
  - [17] A.H. Bougourzi, M. Couture, and M. Kacir, Stony Brook preprint ITP-SB-96-21 (q-alg 9604019).
  - [18] F.D.M. Haldane and M.R. Zirnbauer, Phys. Rev. Lett. **71**, 4055 (1993).
  - [19] M. Karbach, G. Müller, and A.H. Bougourzi, A. Fledderjohann, K.-H. Mütter, Phys. Rev. B **55**, 12510 (1997).